Technical Note
System Identification of a Rotary-Wing Micro Air Vehicle

Joseph K. Conroy*
Graduate Research Assistant

J. Sean Humbert
Assistant Professor

Darryll J. Pines
Professor

University of Maryland, College Park, MD

For a given aerial vehicle, knowledge of a linearized dynamic model greatly aids the development of observers for state estimation and controllers for automation. However, a linearized model consists of stability and control derivatives that can be difficult to obtain from first-principles modeling. This paper presents the identification of a linearized model for a small electric helicopter about the hovering flight condition using control input and kinematic time histories. The methodology utilized frequency response-based system identification and error estimation routines developed at the Army Aeroflightdynamics Directorate located at Moffett Field, California.

Nomenclature

a	longitudinal flapping angle, rad
b	lateral flapping angle, rad
p, q, r	body-fixed roll, pitch, and yaw rates, rad/s
u, v, w	longitudinal, lateral, and heave translational velocities, m/s
$\mu_{\text{lat}}, \mu_{\text{lon}}, \mu_t, \mu_y$	lateral, longitudinal, throttle, and yaw inputs
ϕ, θ	inertial-fixed roll and pitch angles, rad
Ω_{mr}	main rotor rotational velocity, rad/s

Introduction

"Micro air vehicles" (MAV) are small unmanned flying vehicles considered to be significantly smaller than those in the current field of mature unmanned aerial vehicles (UAVs). It is envisioned that such vehicles will eventually be able to autonomously navigate close to the ground in densely cluttered environments. Rotary-wing MAVs are ideal platforms for this scenario as they are capable of hovering and slow-speed flight. This research focuses on the advancement of rotary-wing MAV control and navigation through a better understanding of the vehicle dynamics. A typical approach to autonomous operation of a rotary-wing MAV requires sensing, processing, feedback control, and state estimation. The feedback control and state estimation strategies employ a dynamic model of the vehicle to aid the calculation of the current states and control inputs that are required to regulate the vehicle.

Because of a lack of understanding of low-Reynolds-number aerodynamics, there is a question as to how well-traditional helicopter flight dynamics models would perform if applied to drastically scaled-down vehicles. Furthermore, estimation of inertia parameters and generated forces for model-scale vehicles is tedious and error-prone. Utilizing an alternative approach, this paper presents the identification of a linearized flight dynamics model of a model-scale helicopter about the hover condition utilizing recorded inputs and kinematics. Kinematic motion was recorded using a camera-based visual tracking system. The identification methodology utilized frequency responses to estimate transfer functions between inputs and outputs. The frequency response method was based on prior work of Tischler and Cauffman (Ref. 1) and Mettler et al. (Ref. 2) for larger vehicles, including the identification of BO-105 dynamics and the Yamaha R-50 dynamics. Frequency response analysis was performed using the Comprehensive Identification of FRequency Responses (CIFER®) software developed at the U.S. Army Aeroflightdynamics Directorate (AFDD) located at Moffett Field, California.

Experimental Setup

Flight test vehicle

The flight vehicle was a commercially available, scale-model helicopter (model: Honeybee; manufacturer: Esky Hobby), shown in Fig. 1, having a main rotor 50.5 cm in diameter and a tail rotor 14.5 cm in diameter. The vehicle was modified to include custom avionics (Ref. 3) designed to provide the central interface between the pilot's commands, on-board sensors, and the actuators, as well as telemeter flight data back to a ground station for collection. The control uplink rate was 50 Hz, which was limited by the transmission rate of the RC transmitter (Spektrum). The final gross vehicle weight including the custom electronics was 390 g.

Inputs and kinematic data collection

The time history of the flight kinematics, including the inertial position and orientation of the vehicle, was recorded at 350 Hz using a retroreflective marker-based, eight-camera visual tracking system

*Corresponding author; email: conroyj@umd.edu.
Manuscript received February 2008; accepted September 2010.

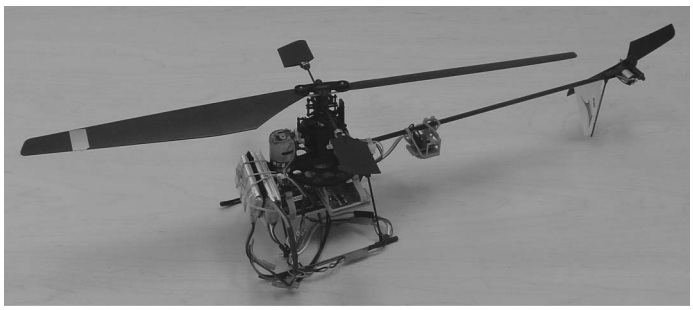

Fig. 1. Test flight vehicle.

(Vicon Motion Systems). A ground control station setup to receive and record concurrently time-stamped control and inertial sensor data was designed in LabVIEW™. The RC transmitter, operated by the pilot, uplinked actuator commands directly to a receiver integrated onto an on-board avionics board. Feedback tends to obscure the natural dynamics of a system; therefore, a minimal amount of feedback was applied in the yaw degree of freedom to make the vehicle pilotable. In addition, the recorded yaw input sent to the ground station was tapped after the feedback was computed to record the actual input to the system.

In addition, the rotor speed, Ω_{mr}, was estimated from the numerical derivative of the rotor Euler yaw angle estimate. Observation of Ω_{mr} was useful to the identification of the heave dynamics for this vehicle, as the main rotor thrust is directly affected by Ω_{mr} rather than the more traditional collective blade pitch control. The visual tracking system fits a rigid body to the collection of points, representing the rotor; however, the amount of blade deflection, due to both coning and cyclic actuation, prevented the consideration of the rotor as a true rigid body system. Therefore, the roll and pitch orientation of the rotor was not considered during the analysis. The inertial positions were also not useful for the subsequent analysis. To summarize, the kinematic states made available to the identification process are given in Eq. (1):

$$y = [\, p \;\; q \;\; r \;\; \phi \;\; \theta \;\; \psi \;\; u \;\; v \;\; w \;\; \Omega_{\text{mr}} \,]^T \tag{1}$$

Nothing was presumed to be known about what forces or deflection angles were generated given a change in the actuator; therefore, all control inputs were simply normalized. The cyclic commands are represented by μ_{lat} and μ_{lon} for lateral/roll inputs and longitudinal/pitch inputs, respectively. These inputs were normalized such that $\mu_{\text{lat}} \in [-1, 1]$ and $\mu_{\text{lon}} \in [-1, 1]$, whereas the tail input, μ_y, and main rotor input, μ_t, were normalized such that $\mu_y \in [0, 1]$ and $\mu_t \in [0, 1]$.

Flight Test Data

Piloted maneuvers were performed to excite the vehicle over a range of frequencies. All flight testing was performed within the capture volume of the visual tracking system. Low-frequency inputs generally lead to large translations; hence, the physical capture area limited the lowest frequency inputs possible. In addition, the inherent high responsiveness of the vehicle made long, unbroken frequency sweeps difficult. Flight data sufficient for identification were possible via the concatenation of a series of "doublet" style inputs and short chirp-like frequency bursts between periods of returning the vehicle to the center of the testing area.

$$\begin{Bmatrix} \dot{b} \\ \dot{p} \\ \dot{a} \\ \dot{q} \\ \dot{\phi} \\ \dot{\theta} \\ \dot{r} \\ \dot{w} \\ \dot{v} \\ \dot{u} \\ \dot{\Omega}_{\text{mr}} \end{Bmatrix} = \begin{bmatrix} -\frac{1}{\tau_f} & -1 & \frac{B_a}{\tau_f} & 0 & 0 & 0 & 0 & 0 & 0 & 0 & 0 \\ L_b & 0 & 0 & 0 & 0 & 0 & 0 & 0 & L_v & 0 & 0 \\ \frac{A_b}{\tau_f} & 0 & -\frac{1}{\tau_f} & -1 & 0 & 0 & 0 & 0 & 0 & 0 & 0 \\ 0 & 0 & M_a & 0 & 0 & 0 & 0 & 0 & 0 & M_u & 0 \\ 0 & 1 & 0 & 0 & 0 & 0 & 0 & 0 & 0 & 0 & 0 \\ 0 & 0 & 0 & 1 & 0 & 0 & 0 & 0 & 0 & 0 & 0 \\ 0 & 0 & 0 & 0 & 0 & 0 & N_r & 0 & 0 & 0 & 0 \\ 0 & 0 & 0 & 0 & 0 & 0 & 0 & Z_w & 0 & 0 & Z_{\Omega_{\text{mr}}} \\ 0 & 0 & 0 & 0 & g & 0 & 0 & 0 & Y_v & 0 & 0 \\ 0 & 0 & 0 & 0 & 0 & -g & 0 & 0 & 0 & X_u & 0 \\ 0 & 0 & 0 & 0 & 0 & 0 & 0 & 0 & 0 & 0 & T_{\Omega_{\text{mr}}} \end{bmatrix} \begin{Bmatrix} b \\ p \\ a \\ q \\ \phi \\ \theta \\ r \\ w \\ v \\ u \\ \Omega_{\text{mr}} \end{Bmatrix}$$

$$+ \begin{bmatrix} \frac{B_{\text{lat}}}{\tau_f} & \frac{B_{\text{lon}}}{\tau_f} & 0 & 0 \\ 0 & 0 & 0 & 0 \\ \frac{A_{\text{lat}}}{\tau_f} & \frac{A_{\text{lon}}}{\tau_f} & 0 & 0 \\ 0 & 0 & 0 & 0 \\ 0 & 0 & 0 & 0 \\ 0 & 0 & 0 & 0 \\ 0 & 0 & 0 & N_{\mu_y} \\ 0 & 0 & 0 & 0 \\ 0 & 0 & 0 & 0 \\ 0 & 0 & 0 & 0 \\ 0 & 0 & T_{\mu_t} & 0 \end{bmatrix} \begin{Bmatrix} \mu'_{\text{lat}} \\ \mu'_{\text{lon}} \\ \mu'_t \\ \mu'_y \end{Bmatrix} \tag{2}$$

Model Structure

The full-state space model is given in Eq. (2). The structure of the vehicle-state space model was based primarily on prior successful work on the identification of helicopter models (Refs. 1, 4–6). Some characteristics unique to the test vehicle, including the rotational-speed based throttle and yaw control, required a basic model derivation of the linear dynamics from first principles. While the result was a full-state space model of all relevant dynamics, the identification proceeded by analyzing decoupled subsystems independently and concatenating to build the full model.

The model structure for the lateral and longitudinal dynamics is the *hybrid model* structure, initially proposed by Tischler and Cauffman (Ref. 1). This formulation, as opposed to the simpler *quasi-steady* model, accurately captures the coupled rotor/fuselage dynamics and is applicable to a wide range of design configurations. Mettler (Ref. 5) utilized this formulation for the identification of the Yamaha R-50 dynamics and provided further validation that the *hybrid model* formulation was sufficient to capture the relevant dynamics, whereas the *quasi-steady* model proved sufficient only for low frequencies.

As formulated, this model does not account explicitly for the dynamics of the flybar and instead considers the rotor and flybar to be a lumped system, with an effective time constant given as τ_f. The flapping angle states, b and a, describe the flapping angles of the lumped rotor/flybar system. B_a and A_b capture the off-axis dynamics between

Table 1. Honeybee-identified model parameters with Cramer–Rao (CR) error estimate

Parameter	Value	CR (%)	$\bar{I}$ (%)	Parameter	Value	CR (%)	$\bar{I}$ (%)
τ_f	0.15	5.467	1.996	A_{lon}	−0.202	2.455	1.053
B_a	1.55	5.829	1.712	N_r	−0.8786	5.342	2.472
L_b	1273	3.354	1.329	Z_w	−0.6802	6.792	2.784
A_b	−2.82	10.94	3.569	$Z_{\Omega_{\text{mr}}}$	0.170	6.447	2.484
M_a	341.6	2.672	0.9205	$T_{\Omega_{\text{mr}}}$	−6.182	4.362	1.142
L_v	−8.246	10.94	3.569	N_{μ_y}	39.06	4.407	2.189
M_u	3.599	8.497	3.217	T_{μ_t}	1449	5.081	1.576
Y_v	−0.4799	16.44	7.685	Δt_{cyclic}	0.033	7.884	3.550
X_u	−0.5214	23.92	11.18	Δt_{μ_t}	0.1163	1.686	0.602
B_{lat}	0.245	2.408	1.114	Δt_{μ_y}	0.069	2.551	1.187
B_{lon}	0.043	9.280	4.277	g	9.81	–	–
A_{lat}	0.044	7.309	2.974				

flapping states, and L_b and M_a are the rotor moment derivatives, capturing the roll and pitch moments induced by the rotor. The terms L_v and M_u capture the low-frequency unstable phugoid mode of the vehicle. Y_v and X_u are translational velocity aerodynamic damping terms. The primary control derivatives associated with the longitudinal and lateral dynamics are B_{lat} and A_{lon}, which represent the rate of change in cyclic angle to the swashplate given changes in the normalized pilot inputs. B_{lon} and A_{lat} are included to capture the off-axis couplings.

The N_r and N_{μ_y} terms define the first-order dynamic model associated with the yaw rate dynamics. Considering the heave degree of freedom, Z_w is the heave velocity damping term, $Z_{\Omega_{\text{mr}}}$ determines the heave acceleration in response to a change in main rotor speed, and the combination of $T_{\Omega_{\text{mr}}}$ and T_{μ_t} specifies a first-order dynamic model, capturing the main rotor speed in response to a change in the throttle input. The control inputs are primed in Eq. (2), indicating that these inputs include the pure delays presented in Table 1. The $\Delta t_{\mu_{\text{cyclic}}}$ term is the pure delay in seconds for both cyclic actuators. The terms Δt_{μ_t} and Δt_{μ_y} specify the delay for the throttle and yaw motors, respectively.

System Identification

Frequency responses and coherences between the inputs and outputs, as well as the subsequent identification of the stability derivatives, were computed using CIFER®, developed by the AFDD. Given a flight data set with sufficient coherence, the CIFER® software package implements a series of subroutines. Following data acquisition and scaling, the Frequency Response Identification (FRESPID) subroutine is applied using multiple windows of appropriate lengths, which provided transfer function and coherence estimates. Considering recommendations in prior work (Ref. 7), window lengths of 3, 6, 9, 12, and 15 s were used. The typical record length used was about 90–120 s in duration. The record length determines the largest window size that can be used, and the window length determines the lowest frequency that can be observed. A smaller window supports better averaging; however, the largest window determines the lowest frequency that can be computed. For this application, the vehicle dynamics is relatively fast, thus allowing the usage of somewhat shorter time windows than might be used for larger aircraft analysis.

The rotor–fuselage dynamics was assumed to be coupled; hence, the lateral and longitudinal inputs influence the off-axis responses. To account for undesired control correlation, the Multi-Input Conditioning subroutine (MISOSA) was applied to condition the data set, considering the presence of multiple inputs. Following these procedures, the Window Combination subroutine (COMPOSITE) was applied to appropriately combine the multiple responses. The processing and conditioning described above results in the transfer function and coherence estimates used to determine the state space model.

Results

The resulting estimated model compares well with the calculated transfer function estimates, which suggests that all relevant dynamics were captured. An example transfer function comparison for the roll input to roll rate is shown in Fig. 2. The *hybrid* model formulation, including cyclic coupling terms, was required to capture the dual rotor/fuselage resonance peaks observed in this plot. The coherence function, indicating the degree to which the output is linearly related to the input, shows that the assumption of linearity in the plotted frequency range is valid.

The identified state space model parameters, along with the associated error bounds, are presented in Table 1. Percentage error Cramer–Rao (CR) bounds, as computed using CIFER's subroutine DERIVID, are included along with the computed insensitivity ($\bar{I}$) percentages. The CR bounds are theoretical minimum limits for the expected standard deviation σ in the parameters estimates that would be obtained from many experiments (Ref. 7). The X_u and Y_v stability derivatives exhibited the highest uncertainty. Mettler (Ref. 5) also noted relatively high uncertainty for these parameters during the system identification of the Yamaha R-50, suggesting a lack of sufficiently low-frequency content as the cause.

While the Honeybee vehicle exhibits a similar dynamic structure to larger scale helicopters, there are several key differences. The Honeybee

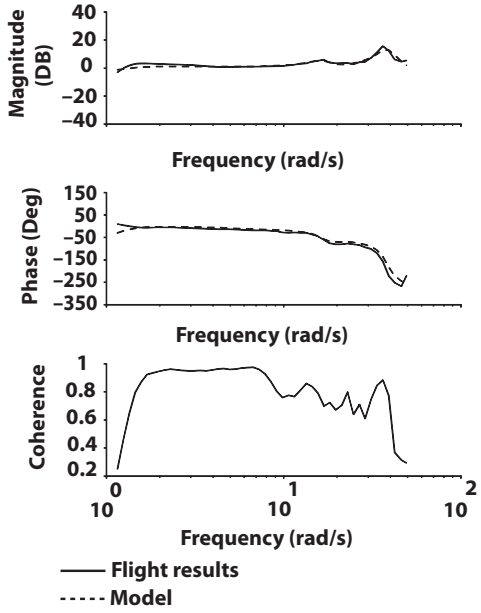

Fig. 2. Roll input to the roll rate.

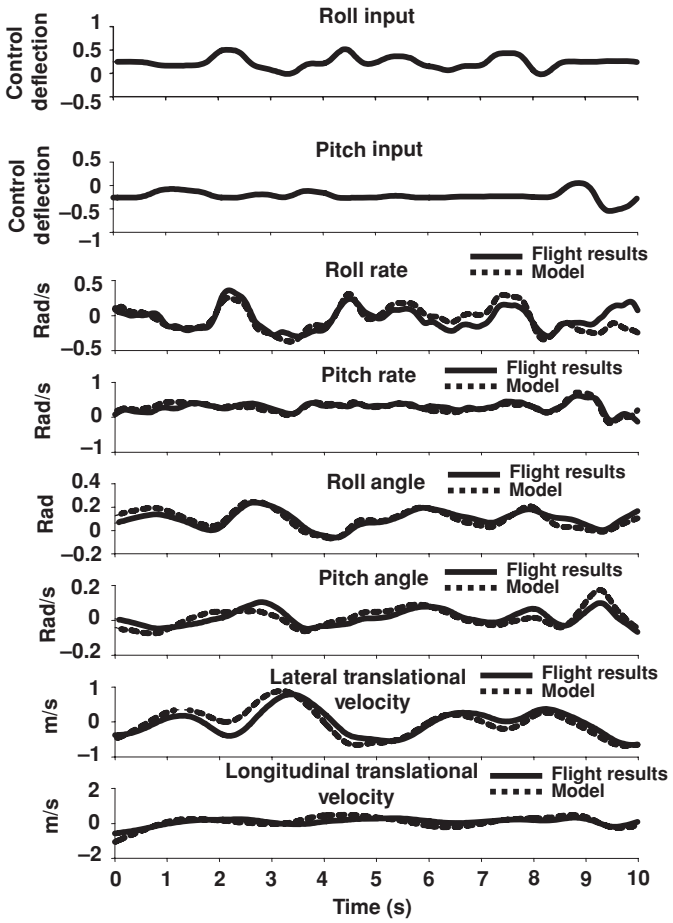

Fig. 3. Lateral input time domain comparison.

dynamics is quick compared to larger counterparts. In part due to the hingeless rotor design, which transmits additional torque to the hub, the control sensitivity is relatively high. Furthermore, the vehicle does exhibit a reasonable degree of cross-coupling, manifested particularly in the control sensitivity matrix. While the vehicle is stabilizable using controllers independently on the roll and pitch axes, performance would benefit from a controller designed to account for this coupling.

Time Domain Verification

Time domain comparisons were performed using the VERIFY subroutine included in the CIFER package to qualitatively evaluate the model performance. The VERIFY subroutine estimates the input and output bias values to minimize the error accumulated by integrating the model numerically. Figure 3, showing the time domain comparison for lateral input excitation, further demonstrates that the relevant dynamics has been captured by the identified model.

Conclusion

(1) A state space model for a small electric helicopter, linearized about hover, was identified using frequency response identification techniques. The resulting model is sufficiently accurate to enable controller and observer design.

(2) A marker-based visual tracking system has been demonstrated successfully as the method of measuring the vehicle kinematics.

(3) The *hybrid model* structure, previously successfully utilized to model the rotor–fuselage interaction on larger vehicles, has been shown to also successfully work for small micro rotorcraft.

Acknowledgments

Thanks to Dr. Mark Tischler of the U.S. Army AFDD for much advice for the identification process. CIFER®, used for frequency domain transfer function estimation, was developed at the U.S. Army AFDD located at Moffett Field, California. This work was supported by an ARO MURI grant with Tom Doligaski serving as contract monitor. Finally, thanks to Evan Ulrich for the design and fabrication of the custom helicopter support structure.

References

[1]Tischler, M., and Cauffman, M., "Frequency-Response Method for Rotorcraft System Identification: Flight Application to BO-105 Coupled Rotor/Fuselage Dynamics," *Journal of the American Helicopter Society*, Vol. 37, (3), 1999, pp. 3–17.

[2]Mettler, B., Tischler, M., and Kanade, T., "System Identification of Small-Size Unmanned Helicopter Dynamics," American Helicopter Society 55th Annual Forum Proceedings, Montreal, Quebec, Canada, May 25–27, 1999, Vol. 2, pp. 1706–1717.

[3]Conroy, J., Samuel, P., and Pines, D., "Development of an MAV Control and Navigation System," Presented at the AIAA Infotech & Aerospace Conference, Arlington, VA, September 26–29, 2005.

[4]Tischler, M B., *Advances in Aircraft Flight Control*, Taylor and Francis, London, 1996.

[5]Mettler, B., *Identification Modeling and Characteristics of Miniature Rotorcraft*, Kluwer Academics Publisher, Norwell, MA, 2003.

[6]Cheng, R. M., Tischler, M., and Schulei, G., "RMAX Helicopter State-Space Model Identification in Hover and Forward-Flight," *Journal of the American Helicopter Society*, Vol. 51, (2), 2006, pp. 201–210.

[7]Tischler, M., and Remple, R., *Aircraft and Rotorcraft System Identification: Engineering Methods with Flight Test Examples*, American Institute for Aeronautics and Astronautics, Reston, VA, 2006.